



STUDY OF THE STRENGTH OF MONOLITHIC CONCRETE LINING OF MINE SHAFT UNDER VARIABLE HEAT LOADS

S.A. Bublik, M.A. Semin, L.Yu. Levin

Mining Institute UB RAS, Perm, Russian Federation

Monolithic concrete is the most popular mine shaft lining type because of its ability to endure rock pressure effects and exclude large deformations of shaft walls. In the case of starting the reverse ventilation mode in the winter season, a significant negative temperature difference may occur between the warm shaft walls and cold air injected from the outside. This temperature difference may have adverse impacts on the concrete lining, inducing high tensile stresses. In this paper, the stress-strain state of the concrete lining and rock mass surrounding the mine shaft are investigated to evaluate the strength of the lining during reverse ventilation mode in winter. In this study, we consider a ventilation shaft with the surrounding concrete lining and rock mass; both solid and concrete are assumed to be isotropic and homogeneous, and their thermodynamic properties are independent of temperature. This allows us to present this scenario as a two-dimensional problem. The temperature drops in the lining and rock mass are believed to be the only significant factor affecting the stress-strain state of the system. When calculating the temperature of both lining and rock mass, the following is taken into account: conductive heat transfer in the rocks and lining, the heat exchange of the lining and rocks with atmospheric air, and the heat exchange of the lining with the mine air. The presence of moisture in rock mass is not considered. Numerical simulation results indicate that the concrete lining is more exposed to tensile stresses acting in the vertical direction. The width of the pre-fracture zone of the lining nonlinearly depends on the duration of the reverse ventilation mode. It was found that with an increase in the air temperature in the shaft, the width of the pre-failure zone of the lining decreases, and the permissible duration of the reverse mode significantly increases.

Key words: mine shaft, concrete lining, temperature deformations, theory of elasticity, strength, numerical simulation

1. Introduction

Currently, the most common way to increase the strength of vertical mine shafts is via the construction of monolithic concrete structures (i.e., linings) along the entire perimeter of the shaft [1, 2]. The lining counters the lateral pressure exerted by the surrounding rocks, thereby protecting shaft walls from possible destruction [3].

The temperature regime of the concrete lining during long-term exploitation of the shaft is primarily determined by the temperature of the air within the shaft [4, 5], which may vary substantially depending on the season.

One of the factors of a sharp and significant change in the air temperature in the shaft can be the reversal of airflow in the mine for the purpose of ventilation. When the reverse ventilation mode is started, the direction of the airflow changes in all (or almost all) mine workings and, in particular, in the shaft. In the event of an emergency (for example, a fire), this ventilation mode makes it possible to remove harmful gases via the shortest route, i.e., through the air supply shafts to the surface, to prevent poisoning of miners [6, 7].

However, in the winter season the reverse mode can create a significant temperature difference between the warm shaft walls and the cold air blown from the outside. This temperature difference may exceed 50 °C (which is most typical of mines in northern latitudes). This is due to the fact that the ventilation shafts are not equipped with air handling systems [8, 9], which would heat the intake air using heat exchangers and allow a predetermined air temperature to be maintained in the shaft. In this situation, a negative temperature difference can adversely affect the shaft lining, resulting in large thermal deformations. The possibility of such a phenomenon is described in [10–12].

Considering that the monolithic concrete lining has a low tensile strength (an order of magnitude lower than that of compression strength) [13], the tensile stresses that arise with a sharp drop in temperature could potentially lead to a dangerous situation where cracking and destruction of the shaft lining occurs. Therefore, the question of determining the maximum permissible temperature changes in vertical mine shafts, i.e., the conditions at which the monolithic concrete lining retains its integrity and load-bearing capacity, becomes more urgent.

The purpose of this work is to study the stress-strain state of concrete lining and rock mass surrounding the mine shaft, and to assess the strength of the concrete lining when reversing the airflow in the mine shaft in the winter season.

2. Formulation of the problem

2.1. Identification of model situation

In this study, we consider a ventilation shaft in the form of a cylinder 8 m in diameter of with surrounding concrete lining and rock mass at a depth interval from 0 to 100 m. We assume that the rock mass and concrete are isotropic and homogeneous.

This assumption is acceptable both for the use in relation to the surrounding rock mass, as this largely comprises basalt rocks with similar thermophysical and mechanical properties at the selected depth interval, and to concrete. Concrete is also considered to be an isotropic and homogeneous material due to the technology used for constructing monolithic concrete linings using formwork (i.e., a homogeneous concrete mixture is placed in the space behind the formwork). Furthermore, due to the limited initial data, the thermodynamic properties of the rock mass and concrete are assumed not to be temperature-dependent. In addition, the condition of frictionless contact at the boundary between the concrete lining and rock mass is assumed. The condition of frictionless contact at the boundary is physically justified by the fact that, in reality, the contact surface is uneven and, as a result, the sliding of concrete relative to rocks is impossible without loss of rock mass continuity [3].

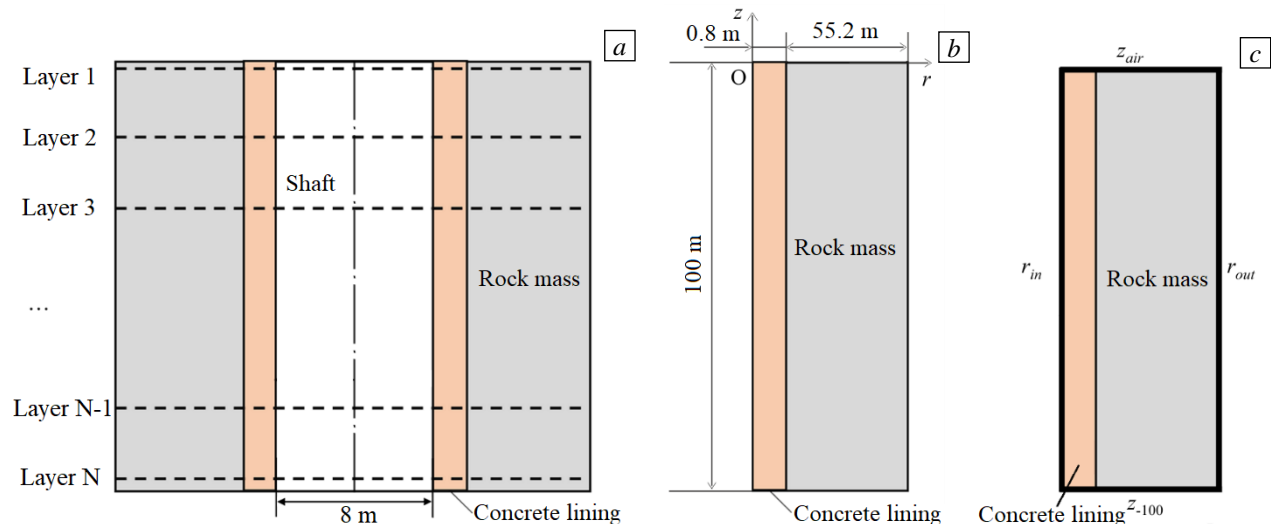


Fig. 1. Schematic representation of the model's (a) geometry, (b) computational domain, and (c) boundary conditions.

The aforementioned hypotheses allow the model to use the property of spatial symmetry, thereby reducing the number of spatial dimensions of the problem to two (Fig. 1). All calculations are performed in a cylindrical coordinate system, $Or\varphi z$.

In this study, the influence of the horizontal pressure of the surrounding rocks is not considered. This is due to the fact that the model is based on the near-surface section of a mine shaft over a relatively small depth, as well as the fact that at these depths the rock mass is represented by hard rock types (basalts) with a relatively low lateral thrust coefficient. As a result of preliminary qualitative assessments, it was found that the lateral pressure on the concrete lining [14] is an order of magnitude smaller than the stresses corresponding to temperature deformations relating to a drop of 50 °C. Thus, the temperature difference at the boundary between the concrete lining and the rock mass is likely to be the only significant factor affecting the stress-strain state of the lining and rock mass. However, it should be noted that this would not be the case when analyzing deeper sections of the shaft.

The analysis of the temperature distribution in concrete lining and rock mass includes the following physical factors: conductive heat transfer in the volume of rocks and shaft lining, heat exchange between the lining, rocks, and the atmospheric air, and heat exchange between the lining and mine air are considered. It is assumed that the rock mass does not contain moisture.

2.2. Heat transfer model in concrete lining and rock mass

To calculate heat transfer in the concrete lining and rock mass, the energy balance equation is used in the following form:

$$\frac{\partial T}{\partial t} = \frac{1}{r} \frac{\partial}{\partial r} \left(a(r) r \frac{\partial T}{\partial r} \right) + a(r) \frac{\partial}{\partial z} \left(\frac{\partial T}{\partial z} \right), \quad (1)$$

where: t — time, s; $T = T(r, z, t)$ — temperature, °C; $a(r) = \frac{\lambda(r)}{c(r)\rho(r)}$ — thermal diffusivity coefficient, m²/s; λ — thermal conductivity coefficient, W/(m·°C); c — specific heat capacity, J/(kg·°C); ρ — density, kg/m³; r — radial coordinate, m; and z — vertical coordinate, m.

The thermal diffusivity coefficient describes the change in thermophysical properties along the radial coordinate (i.e., horizontally) during the transition from the concrete lining to the rock mass. As a result, the coefficient is set using the approximate Heaviside function $H(r)$:

$$a(r) = a_c (1 - H(r - r_{cm})) + a_m H(r - r_{cm}),$$

$$H(r) = 0.001 + \frac{0.999}{1 + \exp(-5r)},$$

where a_c , a_m — thermal diffusivity coefficients of the concrete lining and rock mass, respectively, m²/s; and r_{cm} — radial coordinate of the contact boundary between the concrete lining and rock mass, m.

Such a representation of the Heaviside function is necessary for averaging and smoothing the shaft wall irregularities that are formed during shaft sinking prior to construction of the lining. The function parameters are based on the available data on the irregularities of the shaft walls as a result of penetration; its average value is on the order of ~ 0.1 m.

Equation (1) is supplemented by the following initial and boundary conditions:

$$T|_{t=0} = T_0(z),$$

$$\left. \frac{\partial T}{\partial r} \right|_{r=r_{in}} = \frac{\alpha_s}{\lambda} (T_s(z) - T), \quad T|_{r=r_{out}} = T_0(z), \quad (2)$$

$$\left. \frac{\partial T}{\partial z} \right|_{z=z_{air}} = \frac{\alpha_a}{\lambda} (T_a(z) - T), \quad \left. \frac{\partial T}{\partial z} \right|_{z=z_{-100}} = 0.$$

where: T_0 — temperature of concrete lining and rock mass in natural conditions, °C; T_s ; T_a — temperatures of the mine shaft air and atmospheric air, respectively, °C; α_s , α_a — heat transfer coefficients through the shaft wall and the boundary with atmospheric air, respectively, W/(m²·°C); r_{in} — radial coordinate of the contact boundary of concrete lining with the shaft, m; r_{out} — radial coordinate of the outer boundary of modeled rock mass, m; z_{air} — vertical coordinate of the heat transfer boundary with atmosphere air, m; and z_{-100} — vertical coordinate of the lower model boundary at a depth 100 m. A visual representation of the boundary conditions in (2) can be seen in Figure 1c.

The atmospheric air temperature is set in the form of a sinusoidal curve of seasonal fluctuations from a maximum value of 18.5 °C in the warmest period to a minimum of -47 °C observed in winter:

$$T_a(t) = -14.25 - 32.75 \sin \left[2\pi \left(\frac{t}{365 \cdot 24 \cdot 60 \cdot 60} \right) + \frac{\pi}{2} \right].$$

Mine air temperature in normal ventilation mode was obtained by solving the network distribution problem of air flow rates and air temperatures in the mine, carried out in the Aeraset software package [15]:

$$T_s(z) = 19.84 - 0.0041z.$$

The temperature of the concrete lining and rock mass in natural conditions is represented by the following relationship (based on experimental data on geothermics) [16]:

$$T_0(z) = -2.53 - 0.024z.$$

The mathematical model of heat transfer described above was used to find the temperature distribution in the shaft lining and rocks during the normal shaft ventilation mode. For the normal mode, the horizontal length of the rock mass domain was taken to be equal to 55.2 m. However, in the case of the reverse mode, the computational domain has a shorter length of rock mass in the radial direction, i.e., 2.3 m. This change in the computational domain when simulating the reverse mode is chosen because the reversal time is short compared to the duration of the operating time of the shaft in the normal ventilation mode. Perturbations of the thermal field, therefore, do not have time to propagate through the rock mass to a significant depth. This geometry is also used in later stages of the study to determine the stress-strain state of the concrete lining and rock mass.

In addition to changing the computational domain, the boundary conditions are corrected when the transition to reverse mode occurs. Namely, the air temperature at the shaft wall is set equal to the atmosphere air temperature, and the temperature at the outer boundary is fixed, based on the value obtained from the calculation in the normal ventilation mode. The latter condition is valid because the change in the temperature field will not have time to propagate to reach the new outer boundary of the rock mass. In other aspects, the mathematical model of heat transfer for normal and reverse modes is the same.

The thermophysical parameters used in the numerical solution of the heat transfer problem are given in Table 1.

Table 1. Thermophysical parameters

Parameter	Units	Value
Shaft diameter	m	8
Concrete lining thickness	m	0.80
Rock mass density, ρ_m	kg/m ³	2720
Rock mass specific heat, c_m	J/(kg·°C)	850
Rock mass thermal conductivity, λ_m	W/(m·°C)	1.95
Concrete lining density, ρ_c	kg/m ³	2400
Concrete lining specific heat, c_c	J/(kg·°C)	880
Concrete lining thermal conductivity, λ_c	W/(m·°C)	1.20
Air velocity in the shaft	m/s	9.12 (normal mode) 7.28 (reverse mode)
Heat transfer coefficient at the shaft boundary, α_s	W/(m ² ·°C)	13.75 (normal mode) 10.98 (reverse mode)
Heat transfer coefficient at the atmosphere boundary, α_a	W/(m ² ·°C)	1.20
Shaft operating time in normal mode	year	6
Maximum shaft operation time in reverse mode	hour	24

Thus, by solving equation (1) together with boundary conditions (2), first for the normal ventilation mode, and then for the reverse mode, it is possible to establish the dynamics of the temperature field of the concrete lining and rock mass. Further, we will use the obtained information to calculate the stress-strain state in the shaft lining and rock mass.

2.3. Mechanical model of concrete lining and rock mass

The problem of determining the stress-strain state is solved in a two-dimensional axisymmetric formulation [17–19]. Symmetry is considered relative to the angular coordinate φ . In this case, the displacement components can be written as follows:

$$u_r = u_r(r, z), \quad u_\varphi = 0, \quad u_z = u_z(r, z), \quad (3)$$

where u_r, u_φ, u_z — radial, angular, and vertical displacements, respectively, m.

The relationship between strains and displacements is expressed under the assumption of linearity of strains, which makes it possible to use the equations of the linear theory of elasticity in the framework of the above axisymmetric formulation:

$$\begin{aligned} \varepsilon_{rr} &= \frac{\partial u_r}{\partial r}, \quad \varepsilon_{\varphi\varphi} = \frac{u_r}{r}, \quad \varepsilon_{zz} = \frac{\partial u_z}{\partial z}, \\ \varepsilon_{r\varphi} &= 0, \quad \varepsilon_{rz} = \frac{1}{2} \left(\frac{\partial u_r}{\partial z} + \frac{\partial u_z}{\partial r} \right), \quad \varepsilon_{\varphi z} = 0, \end{aligned} \quad (4)$$

where ε_{ij} ($i = (r, z), j = (r, z)$) — strain tensor components.

Considering equations (4) and temperature stresses, the equations of state of a solid can thus be written in the following form:

$$\begin{aligned} \sigma_{rr} &= \left(K + \frac{4}{3}G \right) \varepsilon_{rr} + \left(K - \frac{2}{3}G \right) (\varepsilon_{\varphi\varphi} + \varepsilon_{zz}) - 3K\alpha\Delta T, \\ \sigma_{\varphi\varphi} &= \left(K + \frac{4}{3}G \right) \varepsilon_{\varphi\varphi} + \left(K - \frac{2}{3}G \right) (\varepsilon_{rr} + \varepsilon_{zz}) - 3K\alpha\Delta T, \\ \sigma_{zz} &= \left(K + \frac{4}{3}G \right) \varepsilon_{zz} + \left(K - \frac{2}{3}G \right) (\varepsilon_{rr} + \varepsilon_{\varphi\varphi}) - 3K\alpha\Delta T, \\ \sigma_{r\varphi} &= 0, \quad \sigma_{rz} = 2G\varepsilon_{rz}, \quad \sigma_{\varphi z} = 0. \end{aligned} \quad (5)$$

where: σ_{ij} ($i = (r, z), j = (r, z)$) — stress tensor components; K — bulk modulus, Pa; G — shear modulus, Pa; α — linear thermal expansion coefficient, $1/^\circ\text{C}$; $\Delta T = T_{reverse} - T_{normal}$ — temperature difference, $^\circ\text{C}$; T_{normal} — temperature of the computational domain at the time corresponding to the end of the normal ventilation mode, $^\circ\text{C}$; and $T_{reverse}$ — temperature of the computational domain at a given time from the start of the reverse ventilation mode, $^\circ\text{C}$.

Considering the assumption regarding the static state of the concrete lining and rock mass, introduced in Section 2.1, it is also possible to determine the stress-strain state of the lining and rocks using the equilibrium equations:

$$\begin{aligned} \frac{\partial \sigma_{rr}}{\partial r} + \frac{1}{r} \frac{\partial \sigma_{r\varphi}}{\partial \varphi} + \frac{\partial \sigma_{rz}}{\partial z} + \frac{\sigma_{rr} - \sigma_{\varphi\varphi}}{r} &= 0, \\ \frac{\partial \sigma_{rz}}{\partial r} + \frac{1}{r} \frac{\partial \sigma_{\varphi z}}{\partial \varphi} + \frac{\partial \sigma_{zz}}{\partial z} + \frac{\sigma_{rz}}{r} &= 0. \end{aligned} \quad (6)$$

To simplify the solution of equations (6), it is necessary to rewrite both equations in terms of displacements. This can be easily achieved using equations (4) and (5).

When starting the reverse operation mode, the largest temperature difference occurs at the shaft boundary, due to the rapid cooling of the air in the shaft to atmospheric temperature. The change in the temperature field in the shaft and the surrounding rock mass will, therefore, occur mainly in the radial direction. In this scenario, we assume that the temperature change will mainly affect the radial component of displacements and is dependent only on the radial coordinate (this hypothesis will be further tested). Thus, equations (3)–(5) can be written as:

$$u_r = u_r(r), \quad u_\varphi = 0, \quad u_z = 0; \quad (7)$$

$$\varepsilon_{rr} = \frac{\partial u_r}{\partial r}, \quad \varepsilon_{\varphi\varphi} = \frac{u_r}{r}, \quad \varepsilon_{zz} = 0, \quad (8)$$

$$\varepsilon_{r\varphi} = 0, \quad \varepsilon_{rz} = 0, \quad \varepsilon_{\varphi z} = 0;$$

$$\sigma_{rr} = \left(K + \frac{4}{3}G \right) \varepsilon_{rr} + \left(K - \frac{2}{3}G \right) \varepsilon_{\varphi\varphi} - 3K\alpha\Delta T, \quad (9)$$

$$\sigma_{\varphi\varphi} = \left(K + \frac{4}{3}G \right) \varepsilon_{\varphi\varphi} + \left(K - \frac{2}{3}G \right) \varepsilon_{rr} - 3K\alpha\Delta T,$$

$$\sigma_{zz} = \left(K - \frac{2}{3}G \right) (\varepsilon_{rr} + \varepsilon_{\varphi\varphi}) - 3K\alpha\Delta T,$$

$$\sigma_{r\varphi} = 0, \quad \sigma_{rz} = 2G\varepsilon_{rz}, \quad \sigma_{\varphi z} = 0.$$

Based on (9), the equilibrium equations are reduced to a single expression:

$$\frac{\partial \sigma_{rr}}{\partial r} + \frac{\sigma_{rr} - \sigma_{\varphi\varphi}}{r} = 0. \quad (10)$$

The model is supplemented with the boundary conditions for zero radial stresses on the shaft wall and zero radial displacements at the outer boundary of the rock mass:

$$\sigma_{rr}|_{r=r_{in}} = 0, \quad u_r|_{r=r_{out}} = 0. \quad (11)$$

The system of equations (8)–(10) ultimately reduces to a second-order ordinary differential equation with respect to one unknown function (u_r) and two boundary conditions (11), therefore, the problem is defined.

It should be noted that our description initially discussed a two-dimensional formulation of the problem, according to which, in the general case, it is also necessary to take into account two additional boundary conditions — zero shear stresses $\sigma_{r\varphi}$ at the boundary r_{in} and zero angular displacements u_φ at the boundary r_{out} . The above equations, i.e., (7)–(9), indicate that these conditions are also fulfilled.

Equation (10), together with boundary conditions (11), is solved with respect to displacements. This makes it possible to find the field of the u_r component, and, further, using relations (8) and (9), the stress and strain field components can also be calculated.

To assess the strength of a concrete lining when exposed to thermal stresses, the first theory of strength was used, i.e., a dangerous state will occur when the highest absolute value of normal stress exceeds a specified permissible value [13]. This assumption is made as the concrete lining in this study is primarily exposed to tensile stresses due to a decrease in temperature, where, as for concrete structures under compressive stresses, this strength theory is not particularly applicable. The specified permissible value was calculated from the strength of concrete in its uniaxial tension test. Thus, the strength criterion can be written as the following inequality:

$$\sigma_n^{\max} \leq R_p, \quad (12)$$

where σ_n^{\max} — highest normal tensile stress, Pa, and R_p — permissible uniaxial tensile stress, Pa.

If an area of stress arises in the concrete lining at which condition (12) is violated, this area is then considered an area of pre-fracture. We do not consider non-linear processes that may take place in this area. Furthermore, if the width of the pre-fracture zone exceeds a limit of $m\%$ of the thickness of the concrete lining, the situation is then considered dangerous for the load-bearing capacity of the lining (note that the value of the parameter m will be specified later).

Table 2 shows the mechanical parameters used in calculating the stress-strain state and assessing the strength of concrete lining. Due to the lack of available data on the mechanical properties of the surrounding rocks, the bulk modulus and the shear modulus of both the rock mass and concrete are taken to be the same.

Further, using the heat transfer model described in Section 2.1 and the mechanical model formulated in this section, we carried out a numerical simulation of the temperature dynamics and stress-strain state in the concrete lining and rock mass, in particular considering how the beginning of the reverse ventilation mode

affects the strength of the concrete lining. For the numerical calculation, the finite difference method was used. For more details on the numerical implementation of the problem, see Section 3.

Table 2. Mechanical parameters of concrete lining and rock mass.

Parameter	Units	Material	
		Concrete	Rock mass
Bulk modulus, κ	GPa	34.40	34.40
Shear modulus, G	GPa	37.50	37.50
Linear thermal expansion coefficient, α	1/°C	$1 \cdot 10^{-5}$	$6.50 \cdot 10^{-6}$
Permissible uniaxial tensile stress, R_p	MPa	1.56	–
Indicator of violation of the load-bearing capacity of the concrete lining, m	%	50	–

2.4. Construction of a mechanical model of concrete lining and rock mass in the ANSYS software package

In this study, the mechanical model of the concrete lining and the rock mass is based on the assumption that the movement of the concrete lining and rock mass occurs only in the radial direction (see Section 2.2). To check the magnitude of the error of the obtained solution, the stress-strain state was additionally calculated in the ANSYS software package. The ANSYS problem formulation is two-dimensional, axisymmetric, and takes into account displacements based on both the radial and vertical coordinates. As the concrete lining and rock mass are assumed to be in a quasi-static state, the Static Structural module in ANSYS was used to calculate the stress-strain state, into which an external file was loaded containing the temperature field obtained from solving the heat transfer problem by the finite difference method.

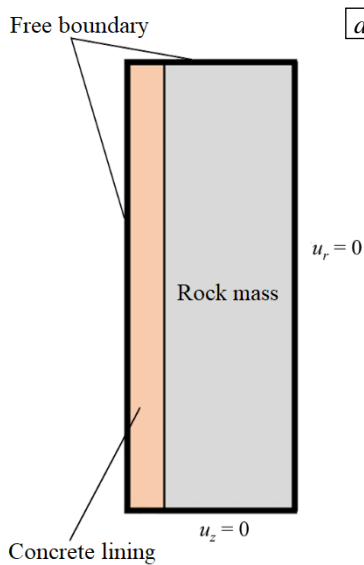


Fig. 2. Mechanical model in ANSYS: schematic representation of boundary conditions (a); computational grid (b).

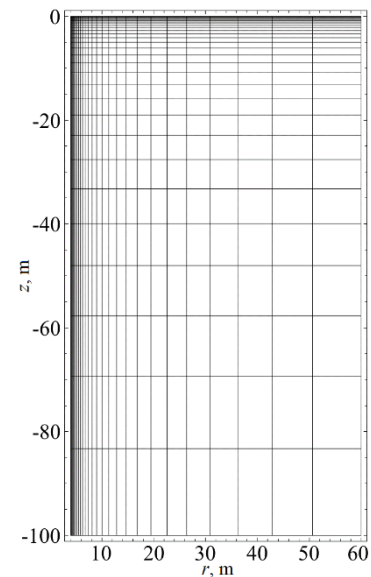
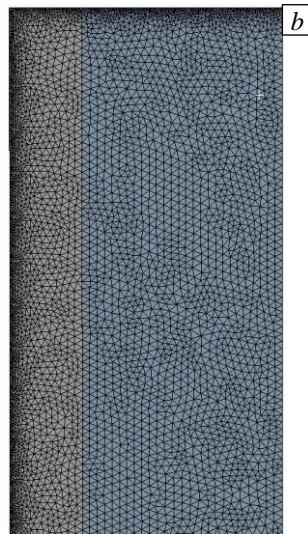


Fig. 3. An example of a computational grid for modeling heat transfer.

The following boundary conditions were applied: the contact surfaces of the concrete lining with the shaft and atmospheric air were considered to be free; the contact surface of the rock mass with atmospheric air was also considered free; and at a depth of -100 m, the normal component of displacements was assumed to be equal to zero (see Fig. 2a). The mechanical properties of the concrete and rock mass were taken from Table 2.

3. Numerical implementation

The dynamics of heat transfer and stress-strain state were determined based on equations (1), (2), and (7)–(11); these equations were solved using the finite difference method. Time discretization was carried out according to the implicit Euler scheme. In the heat transfer problem, the computational domain was covered with a non-uniform regular mesh with an increased density of mesh elements near the boundary of the contact of the concrete lining and the shaft, as well as close to the boundary of heat exchange with the atmosphere (see Fig. 3). When determining the stress-strain state, the grid was uniform. To implement the finite difference method, a specific module was written in the Wolfram Mathematica computer algebra package.

When calculating the stress-strain state in the ANSYS software package, the problem solution area was divided by an irregular and non-uniform mesh of triangular elements with increased element density near the boundary between the concrete lining and the shaft and near the upper boundary with the atmosphere (see Fig. 2*b*).

Table 3 shows the numerical parameters used in the calculation using the module created in Wolfram Mathematica and the ANSYS software package. Notably, the calculations in Wolfram Mathematica require a much smaller number of nodes to solve the heat transfer problem than when determining the stress-strain state. This is a consequence of the fact that for calculating the temperature field, the non-uniform mesh is used with increased density in areas with the highest temperature gradients, which allowed us to significantly reduce the total number of nodes used in the mesh.

Table 3. Parameters of numerical implementation.

Parameter	Dimension	Value
Thermal analysis		
Initial radial coordinate step size	m	0.050 (normal mode) 0.001 (reverse mode)
Initial vertical coordinate step size	m	0.050
Increment factor of the radial coordinate step	%	5
Increment factor of the vertical coordinate step	%	10
Time step	hour	1051.2 (normal mode) 0.48 (reverse mode)
Total number of grid nodes	–	4788 (normal mode) 3306 (reverse mode)
Structural analysis (Wolfram Mathematica)		
Radial coordinate step	m	0.0006
Vertical coordinate step	m	10
Total number of grid nodes	–	50000
Structural analysis (ANSYS)		
Minimum characteristic mesh size	m	0.02
Maximum characteristic mesh size	m	0.08
Total number of grid elements	–	141446

4. Results

Based on the results of numerical calculations of the temperature of the concrete lining and surrounding rock mass, we established that prior to the start of air reversal in the shaft, the highest temperature value (20 °C) was observed at the boundary of concrete lining contact with the shaft (see Fig. 4*a*). Starting the air reversal in the shaft caused the temperature near the shaft wall to drop very quickly, almost reaching the value of the atmospheric temperature. This is due to the intense heat exchange caused by the high air velocity in the shaft (see Fig. 4*b*).

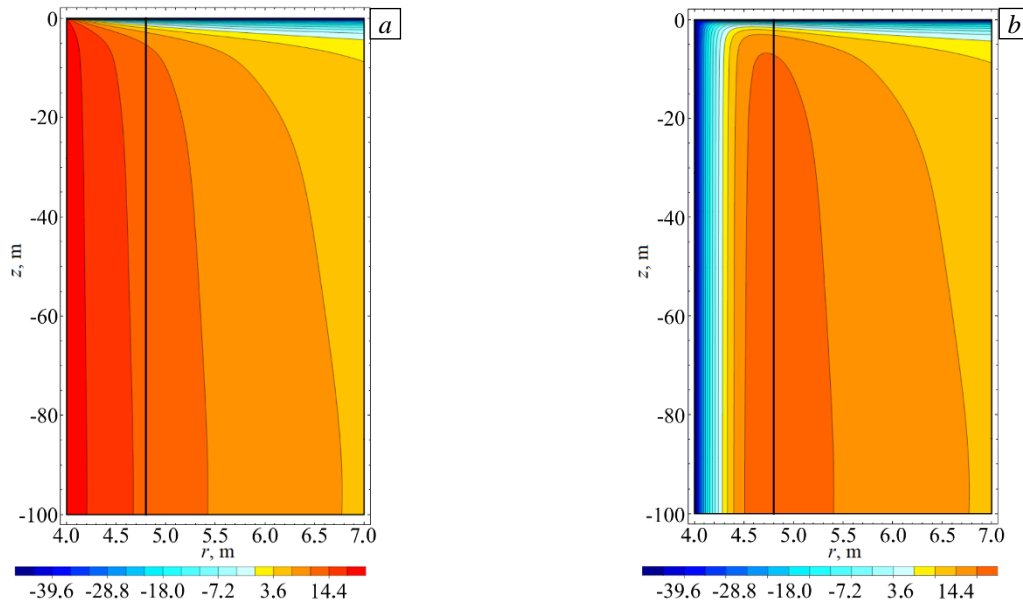


Fig. 4. Temperature field of concrete lining and rock mass (vertical line – contact boundary of concrete lining with rock mass): after (a) 6 years of normal ventilation mode and (b) 24 hours after starting the reverse ventilation mode.

Based on the obtained temperature fields under normal and reversible ventilation modes, we calculated the temperature difference at different time intervals after the onset of reversing the air in the shaft. Calculation data for the area of the concrete lining only are shown in Figure 5. A significant radial temperature gradient is recorded, the highest value of which is observed near the shaft wall. The maximum temperature difference between the initial and calculated states in the area near the shaft wall reaches the value $67\text{ }^{\circ}\text{C}$, 24 hours after starting the reverse flow. The temperature difference at each point of the domain has negative values, i.e., only cooling of the concrete lining and rock mass takes place. The obtained fields also indicate that the isolines of the temperature differences propagate mainly along the radial direction with only minor deviations from vertical orientation near the upper contact boundary with the atmosphere.

Further, the obtained temperature difference was used to calculate the stresses in the concrete lining and rock mass in Wolfram Mathematica. Figure 6 shows the results after 24 hours of reversal; a positive sign of stresses indicates that they are tensile.

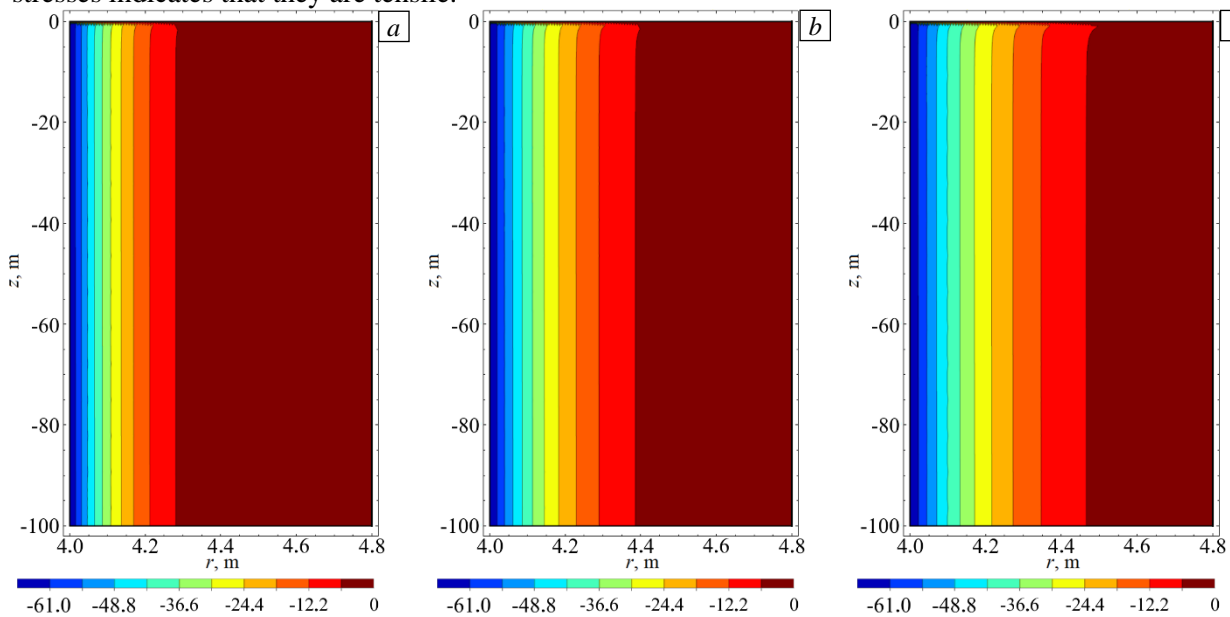


Fig 5. The temperature difference fields in the concrete lining during reversal ventilation mode at different times: after (a) 8 hours; (b) 16 hours; and (c) 24 hours.

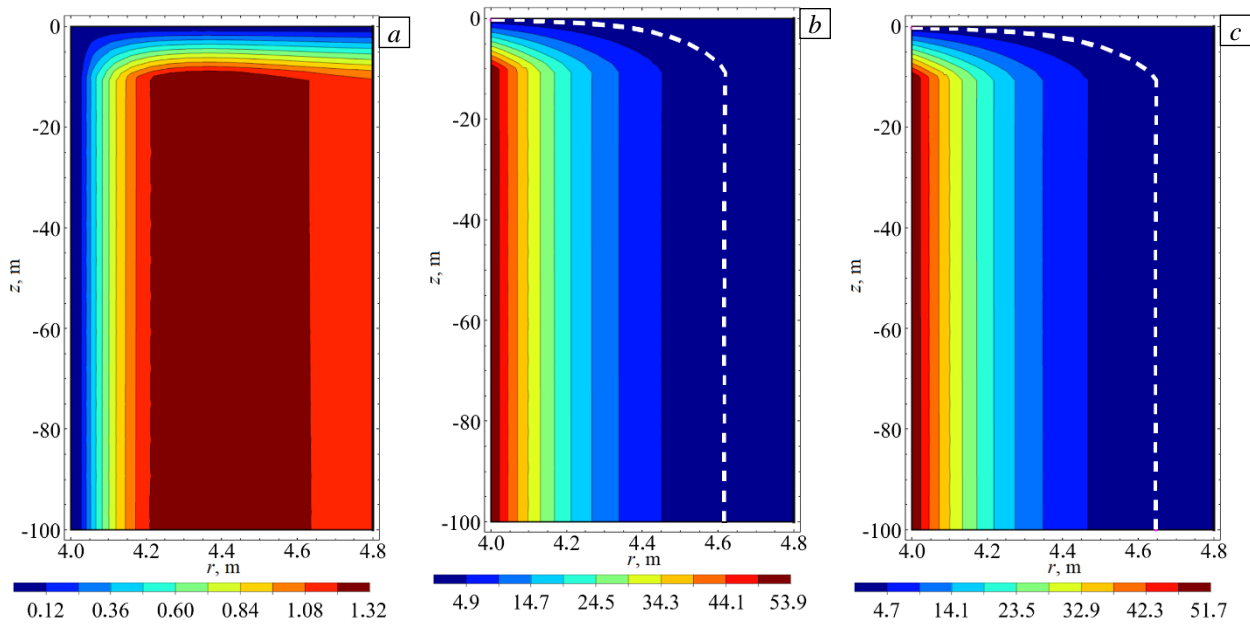


Fig. 6. Stress fields (MPa) in concrete lining after 24 hours of reverse ventilation in terms of: (a) radial σ_{rr} , (b) angular $\sigma_{\phi\phi}$, and (c) vertical σ_{zz} components; the dashed line indicates the boundary of the pre-fracture zone

Based on the fields shown in Figure 6, after 24 hours of air reversal in the shaft, all stresses arising in the computational domain are tensile. When comparing the components, it can be seen that the maximum value of radial stresses (σ_{rr}) is over an order of magnitude lower than the maximum values of angular ($\sigma_{\phi\phi}$) and vertical (σ_{zz}) stresses. In addition, the magnitudes and distributions of the fields of angular and vertical stresses are extremely similar. In this regard, the question arises: can these stresses be considered to be completely equivalent and can either of them be taken as the maximum when assessing the strength of concrete lining according to condition (12)? To answer this question, the boundary of the pre-fracture zone was constructed for angular (Fig. 6b) and vertical (Fig. 6c) stresses; in the case of the vertical stress field, the pre-fracture zone was found to be 4 cm wider than in the field of angular stresses.

Moreover, a more detailed analysis of stress plots along the radial coordinate at a depth of -50 m was carried out (see Fig. 7). As shown, when approaching the contact boundary between the lining and the rock mass angular stresses decrease faster than the vertical ones. In addition, whereas vertical stresses for any reverse ventilation mode duration appear to reach an asymptote, for the angular stresses with reversal times from 2 to 8 hours local areas of compressive stresses can be observed. Thus, on the basis of this analysis, it was decided to take the vertical stress direction as the maximum when assessing the strength of the concrete lining.

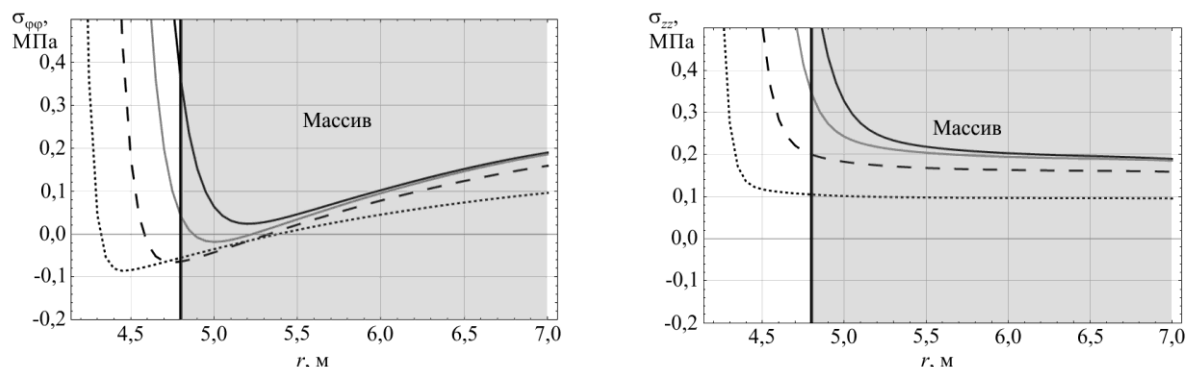


Fig. 7. Dependence of the angular and vertical stresses at a depth of -50 m on the duration of the reverse ventilation mode, hour: — 24, — 16, -- 8, 2

Further, the stress-strain state of the concrete lining and rock mass, as calculated in Wolfram Mathematica, were compared with the results calculated in ANSYS. The stress plots were compared for a reversal duration of 24 hours (see Fig. 8). As shown in Fig. 8b and 8c, the angular and vertical stresses obtained in the calculations in Wolfram Mathematica are almost identical to those found in ANSYS. When

comparing radial stresses (see Fig. 8a), there are significant differences between the two models, however, the differences are more quantitative than qualitative as the distribution of radial stresses is very similar in both cases. The radial stress values obtained in ANSYS are, on average, 1.8 times higher than those calculated in Wolfram Mathematica.

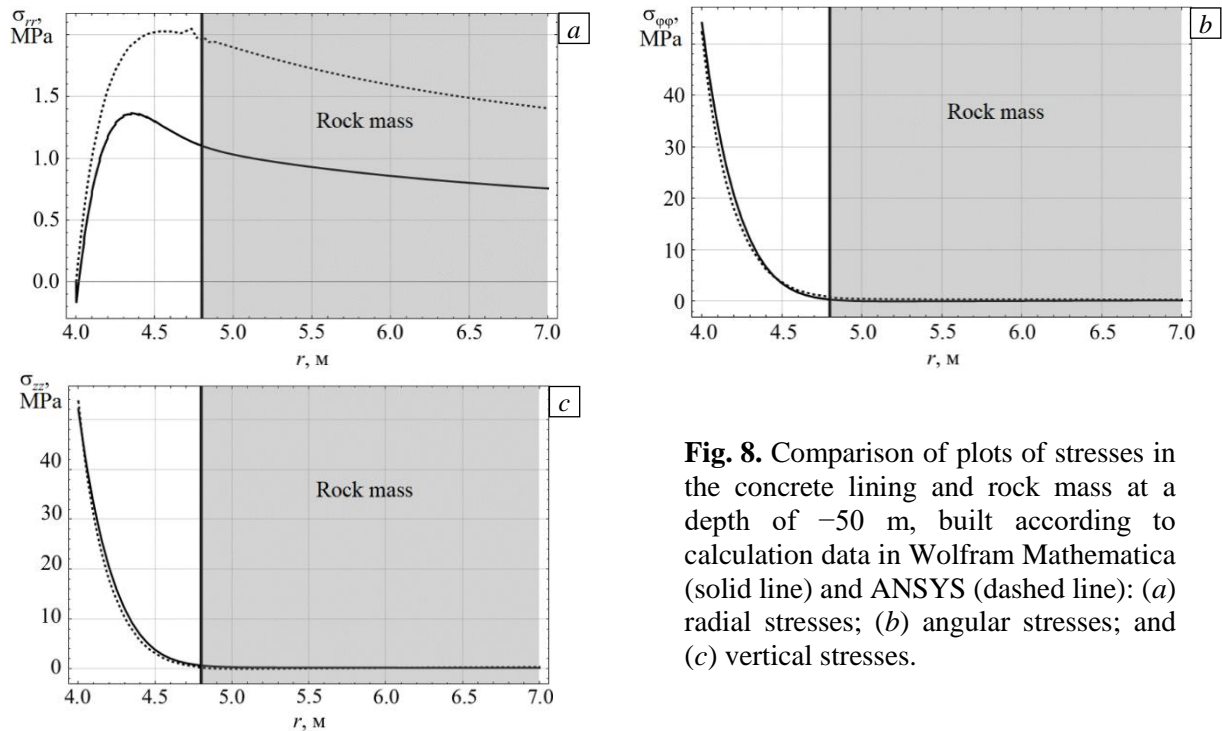


Fig. 8. Comparison of plots of stresses in the concrete lining and rock mass at a depth of -50 m, built according to calculation data in Wolfram Mathematica (solid line) and ANSYS (dashed line): (a) radial stresses; (b) angular stresses; and (c) vertical stresses.

Thus, based on the conditions of the problem being solved, it is possible to use a simplified model for calculating the stress-strain state described by equations (7)–(11). This is demonstrated by the vertical stresses obtained on the simplified basis (used in assessing the strength of concrete lining) being both qualitatively and quantitatively near-identical to calculation data obtained using a full two-dimensional axisymmetric formulation.

Accordingly, based on the obtained results, a plot of the dependence of the width of the pre-fracture zone on the reversal time and different air temperatures in the shaft was constructed (see Fig. 9). As a result of the analysis of Fig. 9, it was found that the width of the pre-fracture zone nonlinearly depends on the duration of the reverse mode. However, even for a short reverse mode duration (no more than 1 hour), the pre-fracture zone width can exceed 0.1 m for all considered values of air temperature. The width of the pre-fracture zone of concrete then increases with an increase in the duration of the reverse ventilation mode for all considered air temperatures in the shaft.

In this study it is assumed that the load-bearing capacity of the concrete lining is violated if the width of the pre-fracture zone reaches $m = 50\%$ of the width of the concrete lining in the radial direction (0.4 m in this problem). Based on the results shown in Fig. 9, a dependence of the maximum permissible reverse mode duration on the air temperature in the shaft was analyzed (see Fig. 10).

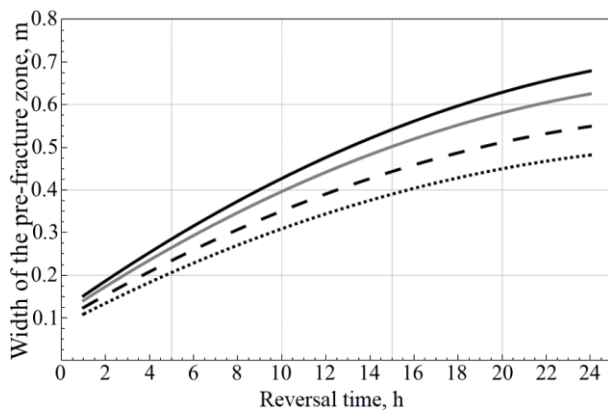


Fig. 9. Pre-fracture zone width vs. duration of reverse ventilation mode for different temperatures of atmosphere air, °C: —47, —28, - -10, 0.

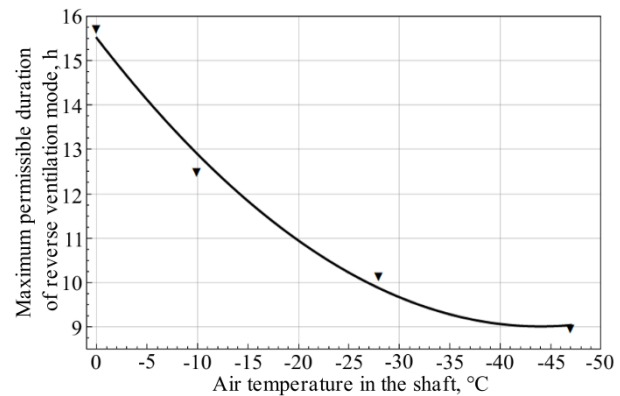


Fig. 10. Maximum permissible duration of reverse ventilation mode vs. air temperature in the shaft.

The resulting plot shows the maximum permissible duration of the reverse ventilation mode for the pre-fracture zone to not exceed 50% of the width of the concrete lining. The increase occurs nonlinearly with increasing temperature (in this case, according to a hyperbolic distribution). With an increase in the air temperature in the shaft from -47 to 0 °C, the maximum permissible duration increases by 57%.

4. Conclusion

Below, we summarize the main results of this work.

1. Two-dimensional thermodynamic and mechanical models of a mine shaft were formulated. These models allow calculating the temperature-dependent stress-strain state of the concrete lining and rock mass. The thermodynamic model includes: conductive heat transfer in the lining and rock mass, heat exchange between the lining and the air in the shaft; heat exchange between the lining and rock mass with the atmospheric air; seasonal fluctuations in atmospheric temperature; and temperature variation when reversing air in the shaft. In the mechanical model, only the effect of the temperature difference on the stress-strain state of the concrete lining and rock mass is considered. The horizontal pressure of the rocks is not considered due to the fact that a near-surface section of the shaft is considered, its vertical length relatively small, and the rock mass is represented by hard rocks with a relatively low coefficient of lateral expansion. The lateral pressure on the concrete lining is not considered, since as a result of the preliminary assessment, the value of the lateral pressure is over an order of magnitude lower than the value of stresses corresponding to temperature deformations at a difference of 50 °C.

2. The results of calculating the stress-strain state of concrete lining based on the temperature factor during air reversal in the mine shaft in the winter season showed that the concrete lining is under tensile stresses to a greater extent and that the maximum absolute values of stresses arise mainly in the vertical direction.

3. Our results indicate that the assumption that the displacements depend only on the radial component and that there are no displacements along the angle and the vertical is valid when assessing the strength of concrete lining. However, it should be noted that in this case, the value of radial stresses decreases by an average factor of 1.8 times.

4. With an increase in the air temperature in the shaft, the width of the pre-fracture zone of the concrete lining decreases; however, the greatest influence on the width of the pre-fracture zone is exerted by a simultaneous increase in both the temperature and the duration of the reversal.

5. A nonlinear dependence on the air temperature in the shaft of the duration of reversal to the state of 50% pre-failure of the lining was obtained. Based on these results, with an increase in the air temperature in the shaft from -47 to 0 °C, the maximum permissible duration of the reversal (i.e., for the pre-fracture zone width to not exceed 50% of the concrete lining width) increases by 57%.

References

1. Kazakevich E.V. *Krepleniye vertikal'nykh stvolov shakht monolitnym betonom* [Fastening of vertical shaft shafts with monolithic concrete]. Moscow, Nedra, 1970. 184 p.

2. Bulychev N.S., Fotiyeva N.N., Strel'cov E.V. *Proyektirovaniye i raschet krepki kapital'nykh vyrabotok* [Design and calculation of support for capital workings]. Moscow, Nedra, 1986. 288 p.
3. Zaslavskiy Yu.Z., Mostkov V.M. *Krepleniye podzemnykh sooruzheniy* [Fastening of underground structures]. Moscow, Nedra, 1979. 325 p
4. Semin M.A., Levin L.Yu. Theoretical research of heat exchange between air flow and shaft lining subject to convective heat transfer. *GIAB – Mining Informational and Analytical Bulletin*, 2020, no. 6, p. 151-167. <https://doi.org/10.25018/0236-1493-2020-6-0-151-167>
5. Kazakov B.P., Levin L. Yu., Shalimov A.V., Zaitsev A. V. Razrabotka energosberegayushchikh tekhnologiy obespecheniya komfortnykh mikroklimaticheskikh usloviy pri vedenii gornykh rabot [Development of energy-saving technologies providing comfortable microclimate conditions for mining]. *Zapiski Gornogo Instituta – Journal of Mining Institute*, 2017, vol. 223, pp. 116-124. <https://doi.org/10.18454/PMI.2017.1.116>
6. Pashkovskiy P.S., Karnaukh N.V., Mavrodi A.V. Health care and safety measures for surface mine locations in underground fire emergency conditions. *Vestnik IZGD – Donbass International Journal of Emergency and Applied Knowledge Management*, 2015, no. 3(3), pp. 8-14.
7. Gendler S.G., Rudakov M.L., Samarov L.Yu. Opyt i perspektivy upravleniya okhranoy truda i promyshlennoy bezopasnost'yu na predpriyatiyakh mineral'no-syr'yevogo kompleksa [Experience and prospects of occupational and industrial safety control in mineral mining and processing]. *Gornyi Zhurnal*, 2015, no. 5, pp. 84-87. <https://doi.org/10.17580/gzh.2015.05.17>
8. Gazizullin R.R., Levin L.Yu., Klyukin Yu.A. Air handling system for mine shaft heating in normal and reverse ventilation modes. *GIAB – Mining Informational and Analytical Bulletin*, 2015, no. S7, pp. 19-25.
9. Kazakov B.P., Shalimov A.V., Semin M.A., Klyukin Yu.A. Matematicheskoye modelirovaniye termodinamicheskikh protsessov v sistemakh vozdukhopodgotovki kaliynykh rudnikov [Mathematical modeling of thermodynamic processes in air conditioning systems in potash mines]. *Gornyi Zhurnal*, 2019, no. 8, pp. 81-84. <https://doi.org/10.17580/gzh.2019.08.16>
10. Prokopov A.Yu. Causes and consequences of origin of heat influence on support and hard armor in air shafts in Donbass. *Izvestiya. vuzov. Severo-Kavkazskiy region. Tekhnicheskkiye nauki – University News. North-Caucasian Region. Technical Sciences Series*, 2007, no. 3, pp. 89-92.
11. Iudin M.M. Treshchinoobrazovaniye v betonnoy krepki vertikal'nykh stvolov rudnikov Severa [Cracking in the concrete lining of the vertical shafts of the mines in the North]. *GIAB – Mining Informational and Analytical Bulletin*, 2007, no. S6, pp. 301-308.
12. Jie Z., Guo-qing Z., Xiang-yu S., Ting L. Numerical simulation on shaft lining stresses analysis of operating mine with seasonal temperature change. *Procedia Earth and Planetary Science*, 2009, vol. 1, pp. 550-555. <https://doi.org/10.1016/j.proeps.2009.09.087>
13. Trapeznikov L.P. *Temperaturnaya treshchinostoykost' massivnykh betonnykh sooruzheniy* [Temperature crack resistance of massive concrete structures]. Moscow, Energoatomizdat, 1986. 272 p.
14. *Rukovodstvo po proyektirovaniyu podzemnykh gornykh vyrabotok i raschetu krepki* [Guidelines for the design of underground mine workings and calculation of the support]. Moscow, Stroyizdat, 1983. 272 p.
15. <https://aeroset.net> (accessed 14 April 2021).
16. Provedeniye kompleksa naturnykh issledovaniy i razrabotka informatsionno-analiticheskoy sistemy nepreryvnogo kontrolya temperaturnogo i napryazhenno-deformirovannogo sostoyaniya prikonturnoy chasti massiva, krepki i armirovki stvola VS-7 rudnika «Taymyrskiy»: otchet o NIR [Carrying out a complex of field studies and development of an information and analytical system for continuous monitoring of the temperature and stress-strain state of the near-contour part of the massif, support and reinforcement of the VS-7 shaft of the Taimyrsky mine: research report]. Perm': GI UrO RAN, 2020. 60 p.
17. Timoshenko S.P., Goodier J.N. *Theory of elasticity*. MacGraw Hill Book Company, 1951. 506 p.
18. Solyanik-Krassa K.V. *Osesimmetrichnaya zadacha teorii uprugosti* [Axisymmetric problem of the theory of elasticity]. Moscow, Stroyizdat, 1987. 336 p.
19. Skripnyak V.A., Skripnyak E.G. *Metody resheniya ploskikh zadach lineynoy teorii uprugosti* [Methods for solving plane problems of the linear theory of elasticity]. Tomsk, TGU, 1998. 32 p.

The authors declare no conflict of interests.

The paper was received on 14.04.2021.

The paper was accepted for publication on 08.06.2021.